Cite this article as: Hossain M.S. & Praticò D. (2026). Temporal and Regional Circular RNA Profiling in a Tauopathy Mouse Model: Implications for Tau Pathology and Neurodegeneration, *AgingBio*, *4*, e20260046. doi: 10.59368/agingbio.20260046.

Research Paper

Temporal and Regional Circular RNA Profiling in a Tauopathy Mouse Model: Implications for Tau Pathology and Neurodegeneration

Mohammad Shahadat Hossain[1] **and Domenico Praticò**[2,*]
[1]Department of Neural Sciences, Lewis Katz School of Medicine, Temple University, Philadelphia, PA, USA
[2]PraticoLab, Philadelphia, PA, USA
[*]Corresponding author: praticolabalzheimer@gmail.com
https://doi.org/10.59368/agingbio.20260046
Received: 7/9/2026, Revised: 9/4/2026, Accepted: 9/28/2026, Published: 11/12/2026

MicroRNAs (miRNA) are noncoding RNA that regulate gene expression posttranscriptionally and play an important role in neurodegeneration. Circular RNAs (circRNAs) are single-stranded, covalently closed loop RNA molecules recognized as upstream regulators of miRNA. Previous studies have shown that circRNAs are dysregulated in Alzheimer's and other neurodegenerative diseases. However, a systematic, age- and region-specific circRNA atlas in primary tauopathy is lacking.

To address this gap, we performed comprehensive circRNA sequencing of hippocampal and cortical tissues from a model of human tauopathy, h-Tau mice, at 3, 6, and 12 months of age. Using exploratory differential expression analyses, candidate prioritization across age groups, functional enrichment, and predicted circRNA–miRNA–mRNA network analyses, we prioritized four circRNAs: circ0033491 (*Sez6l*) and circ0013866 (*Abcc1*) in the cortex, and circ0004838 (*Acaca*) and circ0011361 (*Ppp2r2a*) in the hippocampus. Predicted target networks associated with these circRNAs were represented in pathways related to tau phosphorylation, synaptic function, proteostasis, metabolism, neuroinflammation, and RNA processing.

Together, these findings provide region-specific circRNA profiles for the human tau mouse model and prioritize candidate circRNA-associated networks for future investigation. Although based on computational predictions and exploratory analyses, the identified circRNAs and associated pathways provide a framework for future mechanistic and functional studies of tauopathy.

Introduction

Tauopathies, including Alzheimer's disease (AD), progressive supranuclear palsy (PSP), corticobasal degeneration (CBD), and Pick's disease, are disorders characterized by intraneuronal accumulation of hyperphosphorylated tau protein[1,2]. Tau normally stabilizes axonal microtubules, but its aberrant phosphorylation by kinases such as GSK3b, ERK1/2, JNK, and p38 MAPK at multiple epitopes (Thr181, Thr231, Ser202, Ser396, and Ser422) causes its detachment, somatodendritic mislocalization, and aggregation into insoluble filaments that then become neurofibrillary tangles[3–6]. Tau pathology propagates in a circuit-dependent manner, originating in the entorhinal cortex and hippocampal CA1 before advancing outward through interconnected cortical networks as defined by the Braak staging framework[7,8], with the hippocampus and cerebral cortex representing the two regions of greatest vulnerability.

Noncoding RNAs have emerged as critical posttranscriptional regulators of gene expression in the brain, with microRNAs (miRNAs), short ~22-nucleotide regulatory RNAs that suppress target mRNA translation or promote degradation[9], playing an important role in neurodegeneration. Dysregulated miRNA profiles have been documented in AD brain tissue and biofluids[10–13]. Our group previously profiled miRNA expressions in the cortex and hippocampus of a mouse model of tauopathy, h-Tau mice, across disease progression, revealing distinct region- and age-specific miRNA signatures[14].

Circular RNAs (circRNAs), covalently closed RNA molecules generated by back-splicing of pre-mRNA exons[15], are now recognized as major upstream regulators of miRNA. Their closed-loop architecture confers exceptional metabolic stability in postmitotic neurons, and the brain expresses thousands of circRNA species in a cell type-specific fashion[3,16]. Critically, circRNAs function as competitive endogenous RNA (ceRNA) sponges, sequestering miRNAs through tandem miRNA response elements and thereby de-repressing the cognate target mRNAs[17–19].

Dysregulated circRNA profiles have been described in AD cortex[20] and Parkinson's disease substantia nigra[21,22], but a systematic, age- and region-specific circRNA atlas in primary tauopathy, a condition where tau is the only pathologic feature, is lacking. To address this gap, we performed comprehensive circRNA sequencing of hippocampal and cortical tissues from h-Tau mice, a model of primary tauopathy, at 3, 6, and 12 months of age. We identified circRNA–miRNA sponging networks that

 Copyright © 2026 by the Aging Biology
This is an open access article under the CC BY-NC-ND license (http://creativecommons.org/licenses/by-nc-nd/4.0/).

regulate key disease-associated pathways, including tau phosphorylation and dephosphorylation[23], epigenetic modifications[24], glutamatergic and GABAergic synapses, and microglial efferocytosis[25].

Our findings support the novel hypothesis that specific circRNAs have the potential to be used not only as biomarkers but also as therapeutic targets against tau-driven neurodegeneration.

Materials and Methods

Animals and tissue collection

Human tau (hTau) transgenic mice (JAX #005491) were used in this study. Animals were grouped into three age cohorts (3, 6, and 12 months; n = 4 per group, including 2 males and 2 females). Mice were housed under standard laboratory conditions with ad libitum access to food and water on a 12 h light/dark cycle. All procedures were approved by the Temple University Institutional Animal Care and Use Committee (IACUC) and conducted in accordance with National Institutes of Health guidelines. Following euthanasia by CO inhalation, mice were perfused with ice-cold phosphate-buffered saline. Brains were rapidly removed, and the hippocampus and cerebral cortex were dissected on ice, snap-frozen on dry ice, stored at −80 °C, and shipped to Novogene for RNA isolation, circRNA sequencing, and primary bioinformatics processing.

RNA isolation, library preparation, and sequencing

Total RNA was isolated by Novogene using standard protocols for circRNA sequencing. RNA concentration was measured using a Qubit Fluorometer, RNA integrity was assessed using the Agilent 5400 system, and sample quality was further evaluated by agarose gel electrophoresis. All samples met quality-control criteria for library preparation (RIN range: 7.3–9.0).

circRNA libraries were generated following rRNA depletion and RNase R treatment to enrich circRNAs. Libraries were prepared using strand-specific protocols involving RNA fragmentation, cDNA synthesis, end repair, adapter ligation, PCR amplification, and purification. Library quality was assessed using Qubit, insert-size analysis, and qRT-PCR. Sequencing was performed on an Illumina platform to generate paired-end reads.

Read processing, circRNA identification, and differential expression analysis

Raw reads were processed using FASTQ (v0.23.1) to remove adapter-contaminated reads, reads containing >10% ambiguous nucleotides and reads with >50% low-quality bases (Phred score <5). Clean reads were aligned to the reference genome using HISAT2 (v2.2.1).

circRNAs were identified using both Find_circ v1.2 and CIRI2 v2.0.6 and quantified using back-splice junction (BSJ) read counts and reported as transcripts per million (TPM) for expression profiling and visualization. We acknowledge that TPM normalization has limitations for circRNA analyses because BSJ reads do not represent full-length transcripts, and circRNAs do not fully conform to the transcript-length assumptions underlying conventional TPM calculations. Differential expression analyses were performed using DESeq2 v1.42.0 on count-based data. P-values were adjusted using the Benjamini–Hochberg false discovery rate (BH-FDR) procedure separately for each comparison.

The following comparisons were analyzed: cortex (3M vs. 6M), cortex (3M vs. 12M), hippocampus (3M vs. 6M), and hippocampus (3M vs. 12M). No circRNAs remained significant after BH-FDR correction. Therefore, subsequent analyses were conducted as an exploratory candidate-prioritization approach using nominal $p < 0.05$ and $|\log FC| > 2$. To reduce false-positive findings, circRNAs were additionally required to meet these criteria in both age comparisons within the same brain region. Complete differential expression results, including nominal and BH-adjusted p-values, are provided in **Supplementary Information S1**.

Candidate circRNA selection

Four circRNAs were prioritized for downstream analyses, including one upregulated and one downregulated circRNA from each brain region. Prioritization was based on expression patterns across age comparisons, magnitude of expression change, and exploratory functional annotation analyses.

circRNA–miRNA–mRNA interaction prediction

circRNA–miRNA interactions were predicted using miRanda, and putative miRNA–mRNA interactions were predicted using miRDB. Predicted interactions were incorporated into downstream enrichment analyses and network visualization using Cytoscape v3.10.4.

Functional enrichment analysis

Functional enrichment analyses of circRNA host genes and predicted miRNA target genes were performed using DAVID Bioinformatics Resources. Gene Ontology (GO) Biological Process (BP), Molecular Function (MF), Cellular Component (CC), and Kyoto Encyclopedia of Genes and Genomes (KEGG) pathway analyses were conducted. DAVID uses Fisher's exact test for enrichment and provides Benjamini–Hochberg-adjusted p-values.

Because of the small size of the input gene sets, no GO terms or KEGG pathways remained significant following BH-FDR correction. Consequently, enrichment analyses were treated as exploratory and reported using nominal $p < 0.05$. Both nominal and BH-adjusted p-values are provided in **Supplementary Information S2–S5**.

Region- and age-dependent circRNA expression patterns in tauopathy

To characterize circRNA expression patterns across brain regions and ages, we performed unsupervised hierarchical clustering of all detected circRNAs from the cortex and hippocampus at 3, 6, and 12 months. The resulting heatmap (**Fig. 1A**) showed that samples clustered primarily by brain region, with cortical and hippocampal samples forming distinct groups and biological replicates clustering closely within each condition. As brain regions represented the major source of circRNA variation, age-associated expression changes were subsequently examined within each region separately.

Because no circRNAs remained significant following BH-FDR correction at the current sample size (see the Methods section), candidate circRNAs were prioritized using exploratory thresholds of $p < 0.05$ and $|\log FC| > 2$ (**Fig. 1B–E**). In the cortex, 96 circRNAs were upregulated and 90 downregulated at 6 months relative to 3 months, whereas 60 were upregulated and 126 downregulated at 12 months (**Fig. 1B,C**). In the hippocampus, 75 circRNAs were upregulated and 69 downregulated at 6 months, while 66 were upregulated and 115 downregulated at 12 months compared with 3 months (**Fig. 1D,E**). Across both regions, age-related changes in circRNA expression were more evident at 12 months than at 6 months. These observations should

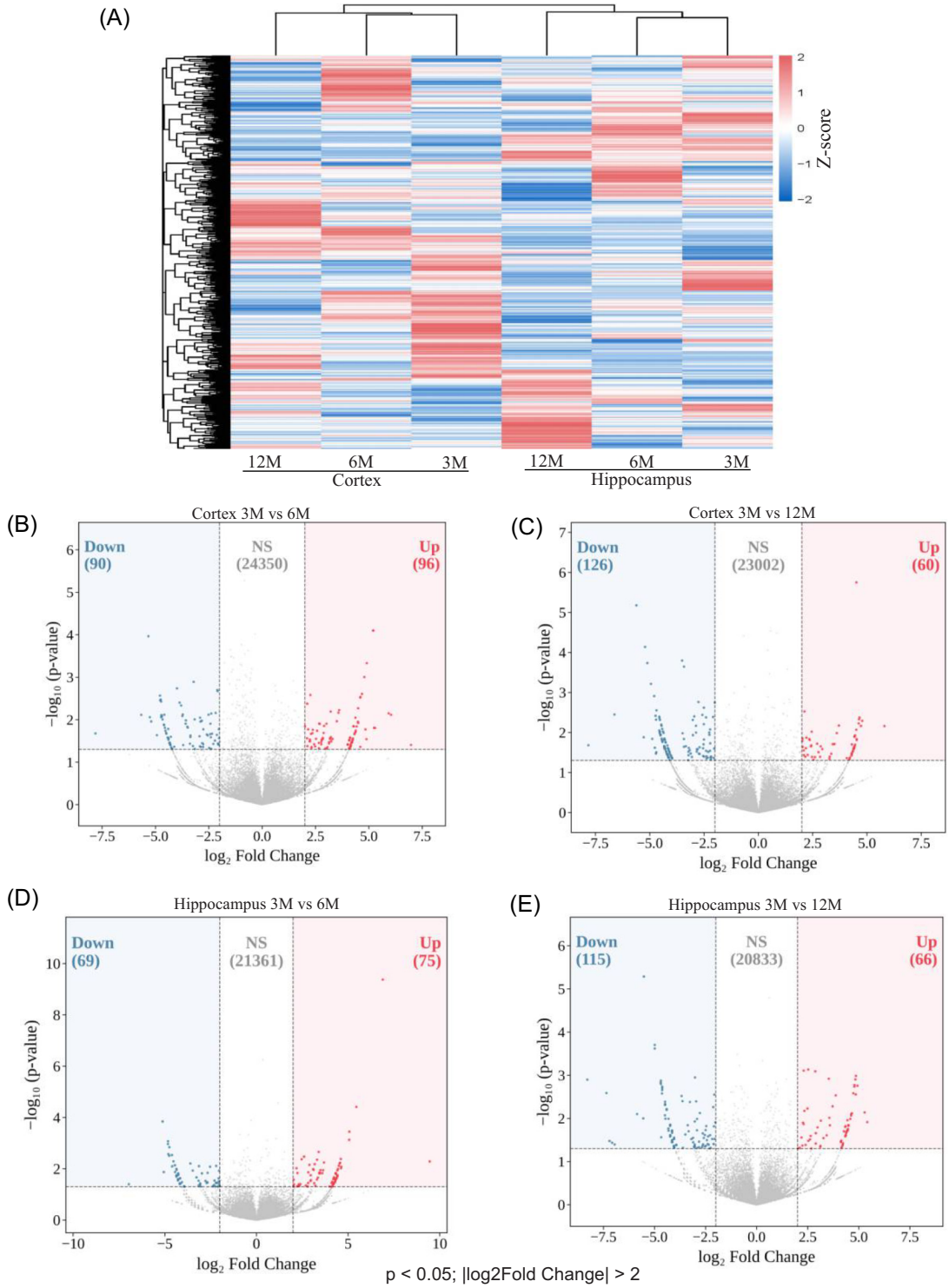


Figure 1. Age-associated circRNA expression patterns in the cortex and hippocampus of hTau mice. (A) Hierarchical clustering heatmap showing circRNA expression profiles in the cortex and hippocampus at 3, 6, and 12 months (3M, 6M, and 12M). Rows represent circRNAs, and columns represent sample groups. Colors indicate z-score-normalized expression values (red, higher expression; blue, lower expression). Volcano plots showing circRNAs meeting exploratory selection criteria ($p < 0.05$ and $|\log FC| > 2$). **(B)** Cortex, 3M versus 6M: increased expression (n = 96), decreased expression (n = 90), and unchanged (n = 24,350). **(C)** Cortex, 3M versus 12M: increased expression (n = 60), decreased expression (n = 126), and unchanged (n = 23,002). **(D)** Hippocampus, 3M versus 6M: increased expression (n = 75), decreased expression (n = 69), and unchanged (n = 21,361). **(E)** Hippocampus, 3M versus 12M: increased expression (n = 66), decreased expression (n = 115), and unchanged (n = 20,833). Red points indicate circRNAs with increased expression, blue points indicate circRNAs with decreased expression, and gray points indicate circRNAs not meeting the selection criteria. No circRNAs remained significant following BH-FDR correction.

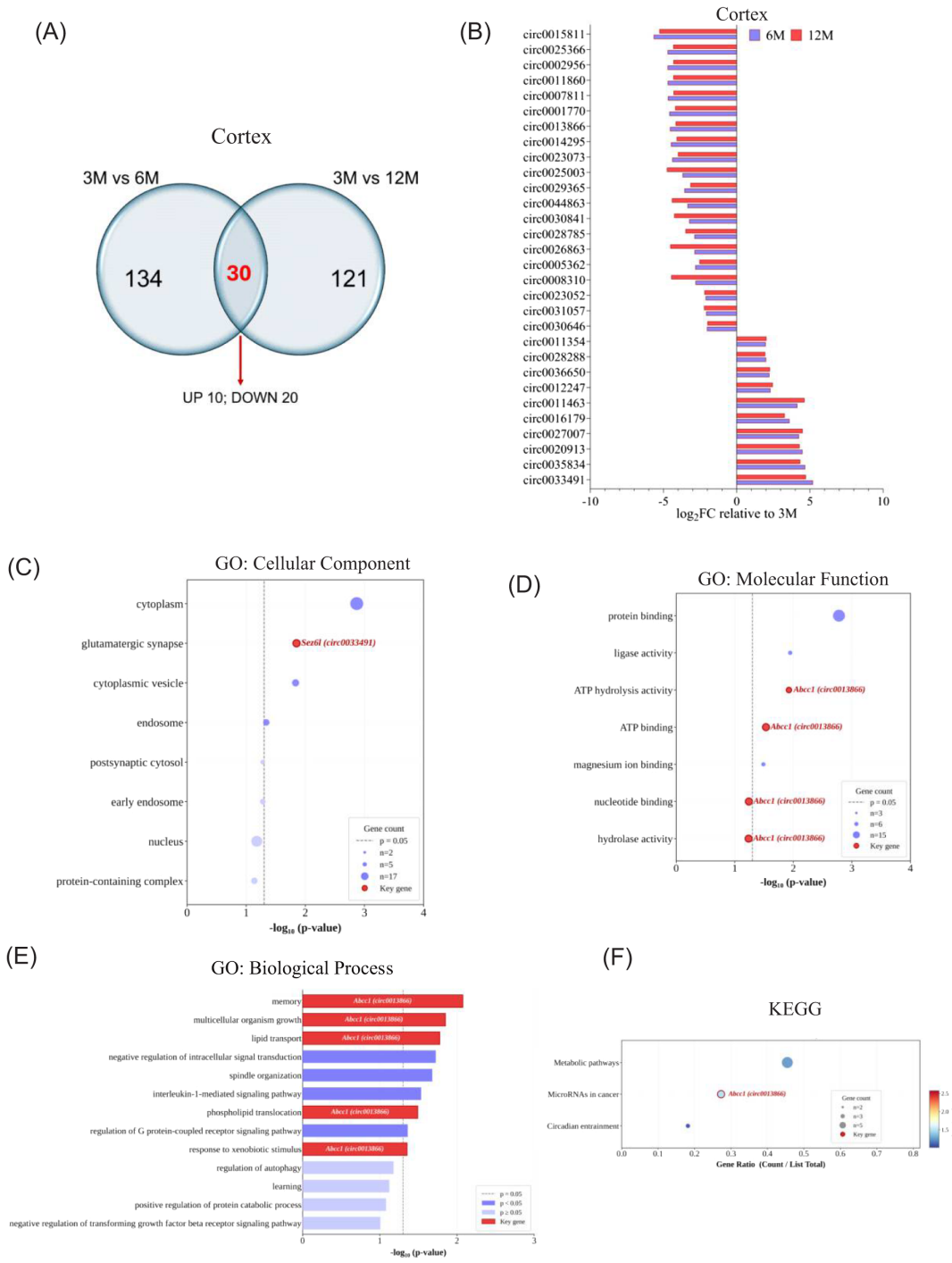


Figure 2. Identification and functional annotation of consistently dysregulated circRNAs in the cortex. (A) Venn diagram showing overlap between circRNAs meeting exploratory selection criteria in the cortex at 3M versus 6M (n = 134) and 3M versus 12M (n = 121). Thirty circRNAs were shared between comparisons, including 10 with increased expression and 20 with decreased expression. **(B)** Log fold-change values relative to 3M for the shared cortical circRNAs at 6M (blue) and 12M (red). **(C–F)** Exploratory GO CC **(C)**, GO MF **(D)**, GO BP **(E)**, and KEGG pathway **(F)** enrichment analyses of parent genes associated with the shared cortical circRNAs. Dot size represents gene count, and color indicates –log (p-value). Selected genes are annotated. Dashed lines indicate p = 0.05. No GO or KEGG terms remained significant following BH-FDR correction.

be considered exploratory and require validation in larger cohorts.

Identification of candidate circRNAs

To identify circRNAs showing expression changes at both 6M and 12M, circRNAs meeting the exploratory selection criteria ($p < 0.05$ and $|\log FC| > 2$) in the 3M versus 6M and 3M versus 12M comparisons were intersected using Venn analysis (Figs. 2A and 3A). In the cortex, 134 and 121 circRNAs were unique to the 6M and 12M comparisons, respectively, whereas 30 were shared (10 increased and 20 decreased). In the hippocampus, 123 and 160 circRNAs were unique to the 6M and 12M comparisons, respectively, whereas 21 were shared (9

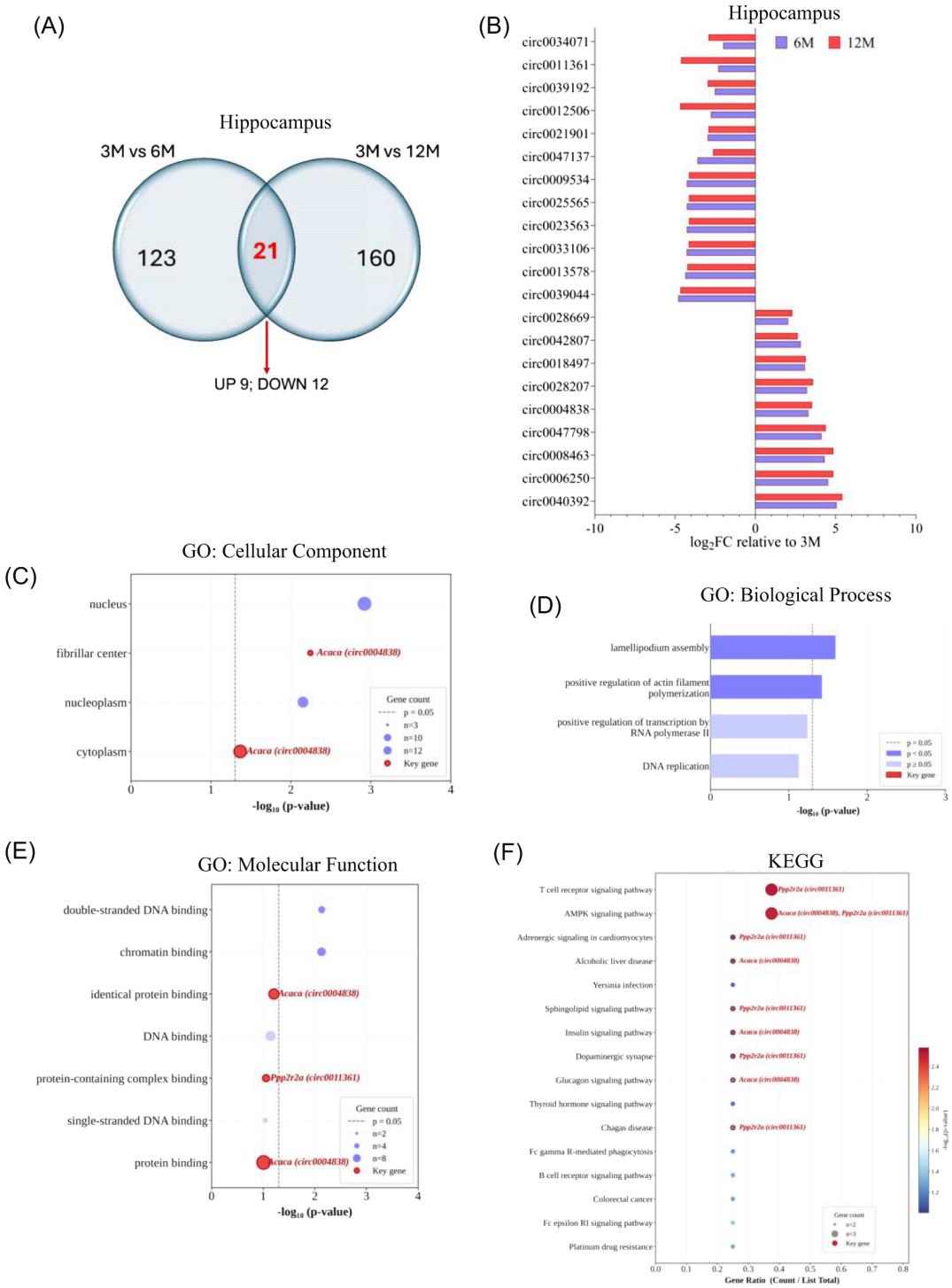


Figure 3. Identification and functional annotation of consistently dysregulated circRNAs in the hippocampus. (A) Venn diagram showing overlap between circRNAs meeting exploratory selection criteria in the hippocampus at 3M versus 6M (n = 123) and 3M versus 12M (n = 160). Twenty-one circRNAs were shared between comparisons, including 9 with increased expression and 12 with decreased expression. **(B)** Log fold-change values relative to 3M for the shared hippocampal circRNAs at 6M (blue) and 12M (red). **(C–F)** Exploratory GO CC **(C)**, GO BP **(D)**, GO MF **(E)**, and KEGG pathway **(F)** enrichment analyses of parent genes associated with the shared hippocampal circRNAs. Dot size represents gene count, and color indicates $-\log_{10}$ (p-value). Selected genes are annotated. Dashed lines indicate p = 0.05. No GO or KEGG terms remained significant following BH-FDR correction.

increased and 12 decreased). The shared circRNAs showed similar directions of change at both time points relative to 3M (Figs. 2B and 3B).

Exploratory enrichment analyses of the parent genes associated with the 30 cortical circRNAs highlighted cytoplasm and glutamatergic synapse categories, with *Sez6l* represented in the latter (**Supplementary Information S6 and S7**). Additional enriched terms included protein binding, ATP hydrolysis activity, memory, lipid transport, multicellular organism growth, and regulation of G protein-coupled receptor signaling (Fig. 2C–E).

KEGG analysis identified the miRNAs in cancer pathway, and *Abcc1* was represented in multiple enriched categories (Fig. 2F).

Exploratory enrichment analyses of the parent genes associated with the 21 hippocampal circRNAs highlighted nucleus and fibrillar center categories, with *Acaca* represented in both (**Supplementary Information S6 and S8**). Additional enriched terms included lamellipodium assembly, actin filament polymerization, double-stranded DNA binding, chromatin binding, and protein-containing complex binding (Fig. 3C–E). KEGG analysis identified T-cell receptor signaling, AMPK signaling, insulin signaling, glucagon signaling, and dopaminergic synapse pathways, with *Acaca* and *Ppp2r2a* represented in the AMPK signaling pathway (Fig. 3F).

Based on expression patterns across time points, magnitude of expression change, and exploratory enrichment findings, four circRNAs were prioritized for further investigation. Among circRNAs showing increased expression, circ0033491 (*Sez6l*) exhibited log FC values of 5.21 and 4.72 at 6M and 12M, respectively, whereas circ0004838 (*Acaca*) exhibited log FC values of 3.31 and 3.53. Among circRNAs showing decreased expression, circ0013866 (*Abcc1*) exhibited log FC values of −4.56 and −4.17, whereas circ0011361 (*Ppp2r2a*) exhibited log FC values of −2.32 and −4.63 at 6M and 12M, respectively (Figs. 2B and 3B). These circRNAs were subsequently prioritized for downstream analyses.

Prediction of circRNA–miRNA–mRNA networks

To investigate potential regulatory interactions involving the four prioritized circRNAs, miRNA binding sites were predicted for circ0033491 (*Sez6l*) and circ0013866 (*Abcc1*) in the cortex and circ0004838 (*Acaca*) and circ0011361 (*Ppp2r2a*) in the hippocampus. Five miRNAs per circRNA were selected based on binding score, minimum free energy, and the presence of multiple predicted binding sites (Table 1).

In the cortex, circ0033491 (*Sez6l*) showed predicted interactions with miR-665-5p (−73.5 kcal/mol; three binding sites), miR-709 (binding score 176; two sites), and miR-6538 (−57.4 kcal/mol; two sites). circ0013866 (*Abcc1*) showed predicted interactions with miR-6902-3p (−39.3 kcal/mol), miR-5624-3p (−35.5 kcal/mol), and miR-7661-5p (binding score 170), each with two predicted binding sites. In the hippocampus, circ0004838 (*Acaca*) contained a cluster of predicted miRNA binding sites between positions 290 and 334, including miR-181a-2-3p, whereas circ0011361 (*Ppp2r2a*) showed predicted interactions with miR-30b-3p (−36.3 kcal/mol; two sites) and miR-6920-5p (−35.3 kcal/mol; two sites).

Putative miRNA–mRNA interactions were predicted using miRDB (**Supplementary Information S9**). Target genes were primarily selected using a miRDB score threshold of ≥80. For two miRNAs, a score range of 55–70 was additionally used to obtain a sufficient number of targets for downstream analyses. The resulting miRNA–mRNA interactions were used for enrichment analysis and network construction.

The predicted circRNA–miRNA and miRNA–mRNA interactions were integrated to construct a circRNA–miRNA–mRNA network. Cytoscape visualization showed a hierarchical network structure in which each circRNA was connected to five prioritized miRNAs and their predicted downstream mRNA targets (Fig. 4).

Exploratory functional enrichment analysis

To explore biological pathways represented among the predicted mRNA targets of each circRNA–miRNA network, GO and KEGG enrichment analyses were performed (**Supplementary Information S2–S5**). Because no GO terms or KEGG pathways remained significant after BH-FDR correction, the enrichment results are presented as exploratory findings and should be interpreted with caution.

Exploratory enrichment analysis of the predicted targets associated with the circ0033491 network highlighted neuronal and synapse-related categories, including growth cone, cell leading edge, glutamatergic synapse, and neuronal cell body. Enriched MFs included ubiquitin protein ligase binding, protein kinase activity, and calcium channel activity. Enriched BPs included regulation of apoptosis, insulin receptor signaling, neuron projection development, calcium ion transport, and ERK signaling. KEGG analysis identified pathways including insulin signaling, MAPK signaling, cell cycle, Hippo signaling, axon guidance, insulin resistance, and AGE-RAGE signaling (**Supplementary Information S2**).

The circ0004838 network was enriched for synapse-associated and kinase-related categories. Enriched CCs included synapse, glutamatergic synapse, postsynaptic density membrane, postsynaptic density, and GABAergic synapse. Enriched MFs included kinase activity, protein tyrosine kinase activity, and transmembrane receptor protein tyrosine kinase activity. BP categories included protein autophosphorylation, peptidyl-tyrosine phosphorylation, synapse organization, and synapse assembly. KEGG analysis identified gap junction, calcium signaling, cholinergic synapse, and estrogen signaling pathways (**Supplementary Information S3**).

The circ0013866 network showed enrichment of neuronal, synaptic, phosphatase-related, and apoptosis-associated categories. Enriched CCs included dendrite, axon, glutamatergic synapse, postsynaptic membrane, and endoplasmic reticulum membrane. Enriched MFs included histone deacetylase binding, cysteine-type endopeptidase activity, and protein tyrosine phosphatase activity. Enriched BPs included nervous system development, cellular response to insulin stimulus, apoptotic process, and intracellular signal transduction. KEGG analysis identified efferocytosis, dopaminergic synapse, retrograde endocannabinoid signaling, GABAergic synapse, and morphine addiction pathways (**Supplementary Information S4**).

The circ0011361 network showed enrichment of synaptic, axonal, and protein-binding categories. Enriched CCs included axon, glutamatergic synapse, synapse, presynaptic membrane, postsynaptic density, and dendritic spine membrane. Enriched MFs included protein binding, metal ion binding, and zinc ion binding. Enriched BPs included nervous system development, positive regulation of neutrophil migration, and axonal fasciculation (**Supplementary Information S5**).

Discussion

The present study provides a region-specific characterization of circRNA expression across aging in the hTau mouse model and identifies circRNA signatures in the cortex and hippocampus. CircRNA expression profiles clustered primarily by brain region rather than age, consistent with previous reports demonstrating a region- and cell type-specific circRNA expression in the brain[26,27]. Altered cortical circRNAs were associated with pathways involved in glutamatergic signaling, lipid transport, and memory-related processes, all of which are involved in early synaptic dysfunction and cognitive decline[3,28,29]. In contrast,

Table 1. Predicted miRNA binding interactions for the four key aging-associated circRNAs, ranked by total binding energy within each circRNA.

circRNA	miRNA	Total Energy (kcal/mol)	Highest Binding Score	Lowest Energy (kcal/mol)	Binding Position(s)	miRNA Length	circRNA Length
circ0033491 (*Sez6l*)	miR-665-5p	−73.50	165	−32.36	232, 532, 400	26	697
	miR-709	−60.91	176	−37.61	40, 470	19	
	miR-6538	−57.43	168	−35.27	432, 399	19	
	miR-3091-3p	−36.05	160	−18.68	403, 535	22	
	miR-686	−35.04	160	−19.54	204, 116	22	
circ0013866 (*Abcc1*)	miR-6902-3p	−39.30	159	−20.30	52, 1	21	441
	miR-5624-3p	−35.48	160	−20.31	415, 163	22	
	miR-6540-5p	−32.39	159	−16.64	414, 163	22	
	miR-7661-5p	−29.77	170	−18.64	168, 209	25	
	miR-12188-5p	−25.10	159	−25.10	201	24	
circ0004838 (*Acaca*)	miR-7211-5p	−27.14	166	−27.14	290	22	360
	miR-7061-3p	−21.73	166	−21.73	295	22	
	miR-181a-2-3p	−22.97	159	−22.97	39	22	
	miR-7094-1-5p	−24.67	163	−24.67	334	23	
	miR-211-5p	−24.02	158	−24.02	294	22	
circ0011361 (*Ppp2r2a*)	miR-30b-3p	−36.31	152	−20.76	358, 597	22	802
	miR-6920-5p	−35.33	157	−20.10	735, 512	22	
	miR-1911-3p	−25.61	160	−25.61	677	22	
	miR-6908-5p	−25.52	170	−25.52	137	22	
	miR-693-3p	−24.33	168	−24.33	578	23	

hippocampal circRNA dysregulation was associated with nuclear organization, cytoskeletal remodeling, and metabolic signaling pathways, including AMPK-mediated energy homeostasis[30,31]. Together, these findings highlight region-specific circRNA expression changes during tauopathy progression.

Furthermore, integrative analysis of circRNA expression, predicted miRNA interactions, and predicted mRNA targets prioritized four circRNAs: circ0033491 (*Sez6l*) and circ0013866 (*Abcc1*) in the cortex, and circ0004838 (*Acaca*) and circ0011361 (*Ppp2r2a*) in the hippocampus. The prioritized circRNA-associated networks included predicted target genes linked to tau phosphorylation (*Gsk3b*, *Map3k9*, *Ppp2r5c*)[32–36], synaptic function (*Gabrb2*, *Snap25*, *Dlgap1*, *Shisa6*)[37–40], proteostasis (*Bag4*, *Ube2k*, *Psmb2*, *Atg4c*)[41–43], epigenetic regulation (*Hdac2*, *Suz12*)[44], and RNA splicing (*Clk2*, *Mbnl1*)[45]. In addition, genes associated with calcium homeostasis and neuronal signaling, including *Itpr1* and *Atp2b*[40,46], receptor tyrosine kinase signaling (*Dyrk1a*, *Epha4*, *Erbb4*, *Pdgfra*)[47–49], metabolic regulation (*Cpt1a*, *Slc16a1*, *Adcy6*, *Acaca*)[50,51], and neuroinflammatory pathways (*Socs7*)[52], were also represented within the predicted networks. Although these interactions remain computationally predicted, the representation of multiple pathways previously implicated in tauopathy suggests that altered circRNA expression may be associated with several BPs relevant to disease progression.

Moreover, upregulated circRNAs were associated with kinase-related pathways, including MAPK, insulin, and PI3K-Akt signaling, whereas downregulated circRNAs were linked to phosphatase-related networks involving PP2A-associated regulators. Given the established role of kinase-phosphatase balance in regulating tau phosphorylation[53–55], these observations suggest that the prioritized circRNAs may be linked to pathways involved in tau phosphorylation homeostasis. Notably, PP2A-associated regulators were represented within the predicted networks, given that reduced PP2A activity is a well-documented feature of AD[56].

Synapses-related pathways were represented across all four prioritized networks. Enriched categories included glutamatergic synapse, postsynaptic density, synaptic transmission, and synapse organization, suggesting that predicted circRNA-associated pathways may be linked to processes involved in neuronal connectivity and signaling. The representation of GABAergic synapse-related pathways within the circ0013866 network is notable given previous reports of GABAergic interneuron dysfunction in AD and related tauopathies[57–59]. Together, these findings are consistent with the established importance of synaptic dysfunction in neurodegeneration[60–62].

Proteostasis-related pathways were also represented across multiple networks. Predicted targets associated with circ0033491 and circ0011361 were enriched for ubiquitin-mediated proteolysis and proteasome-related functions. Representative predicted targets included *Bag4*, *Ube2k*, and *Psmb2*, genes of cellular proteostasis pathways that regulate the balance between proteasomal degradation and autophagy[63,64]. Given the central role of the ubiquitin-proteasome system (UPS) in tau degradation, alterations in these pathways could influence the accumulation of pathological tau species[65,66]. Enrichment of autophagy- and lysosome-related pathways within the circ0004838 network suggests a possible involvement of the autophagy-lysosome system. Consistent with this observation, postmortem studies in AD, CBD, and PSP have reported autophagic and lysosomal abnormalities associated with pathological tau accumulation[67,68]. Similarly, enrichment of pathways associated with histone deacetylation and chromatin remodeling, together with the presence of *Hdac2*

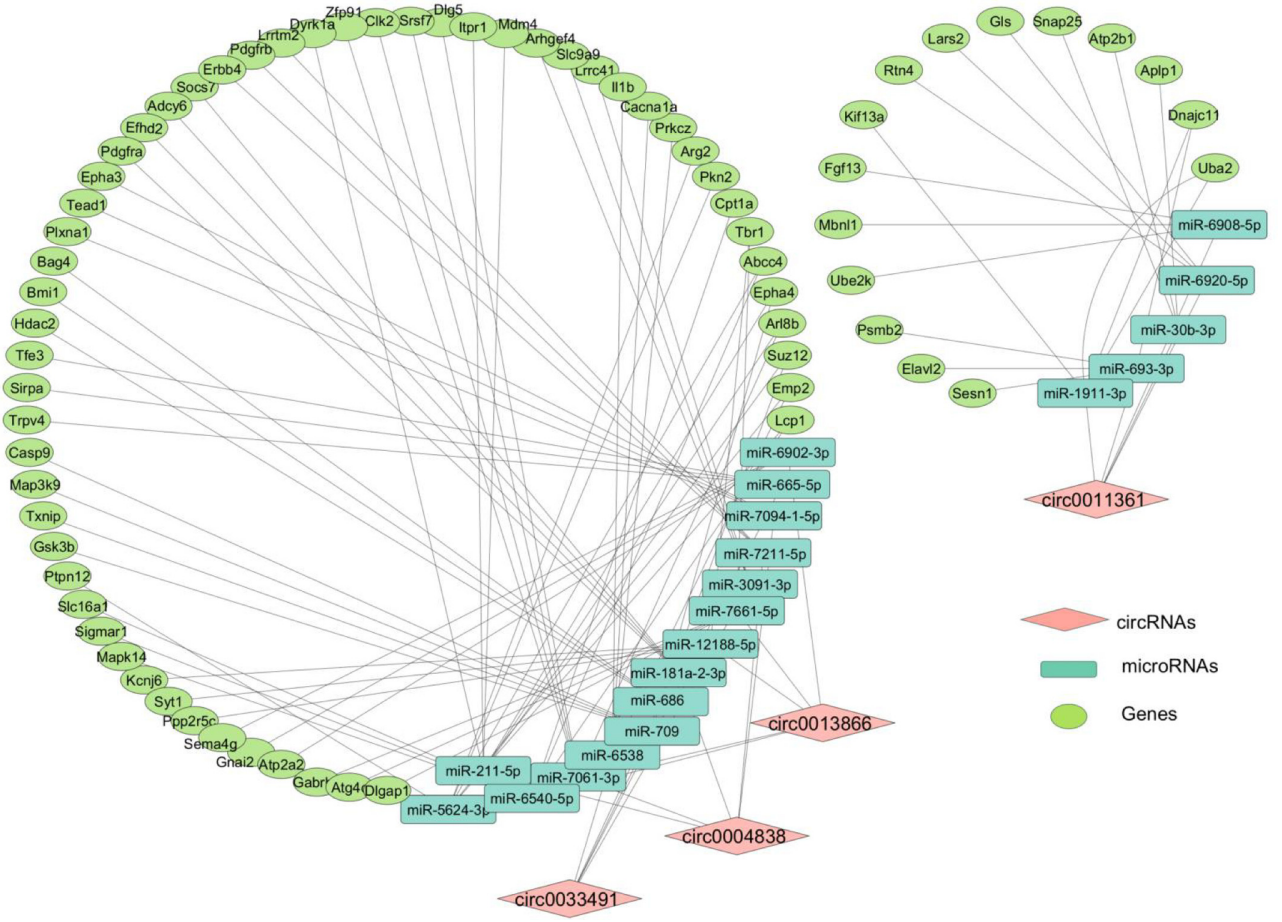


Figure 4. circRNA–miRNA–mRNA regulatory interaction network of key dysregulated circRNAs. Predicted circRNA–miRNA–mRNA networks for four prioritized circRNAs: circ0004838, circ0033491, circ0013866, and circ0011361. Diamond-shaped nodes represent circRNAs, rectangular nodes represent miRNAs, and elliptical nodes represent predicted mRNA targets. Edges represent predicted circRNA–miRNA and miRNA–mRNA interactions. Networks were generated using miRanda and miRDB predictions and visualized using Cytoscape. All interactions shown are computational predictions and have not been experimentally validated.

and *Suz12*, suggests a possible link between circRNA-associated networks and epigenetic regulation. Notably, *Hdac2*, a predicted target of the circ0033491/miR-686 axis, has been implicated in the repression of synaptic plasticity genes in AD[69], while SUZ12, a core component of the polycomb repressive complex 2 PRC2 complex, mediates H3K27me3-dependent transcriptional silencing and has been linked to age- and disease-associated epigenetic regulation[70].

The enrichment of neuroinflammatory pathway components, including TNFa signaling, NF-κB activation through *Zfp91*, interleukin-1β signaling through *Il1β*, and efferocytosis across multiple circRNA target networks, suggests an association between these ceRNA networks and neuroinflammatory processes, a well-established feature of tauopathy[71–74]. Furthermore, the enrichment of efferocytosis-related pathways within the circ0013866 network may indicate involvement of phagocytic clearance mechanisms that have previously been linked to neuroinflammatory responses[75–77].

Another notable observation was the representation of RNA splicing and spliceosome-related pathways within the circ0004838 and circ0011361 networks. Predicted targets included *Clk2*, *Srsf7*, *Mbnl1*, *Srsf1*, and *Elavl2*, all of which have been associated with alternative splicing regulations. Several of these factors, particularly *Clk2*, *Srsf7*, and *Mbnl1*, have been linked to tau exon 10 splicing and regulation of the 4R:3R tau isoform ratio, a defining molecular feature of multiple primary tauopathies ratio[45,78,79]. Their representation within the predicted networks suggests a potential association between circRNA expression changes and molecular pathways involved in tau isoform regulation.

Taken together, these observations support a conceptual framework (**Fig. 5**) in which region-specific circRNA expression changes are associated with distinct but partially overlapping molecular pathways in the cortex and hippocampus. Despite regional differences, multiple predicted networks were associated with pathways related to tau phosphorylation, synaptic function, proteostasis, neuroinflammation, metabolic regulation, and RNA processing. As these relationships are derived from computational predictions and exploratory enrichment analyses, they should be considered hypothesis-generating rather than mechanistic.

Several limitations should be acknowledged. No circRNAs remained significant following BH-FDR correction, and all downstream analyses were therefore based on candidate circRNAs prioritized using exploratory thresholds. In addition, the circRNA–miRNA–mRNA interactions and enrichment analyses were computationally predicted and required experimental validation. The absence of age-matched wild-type controls limits the ability to distinguish tauopathy-associated changes from normal aging effects. Furthermore, the study was designed to evaluate

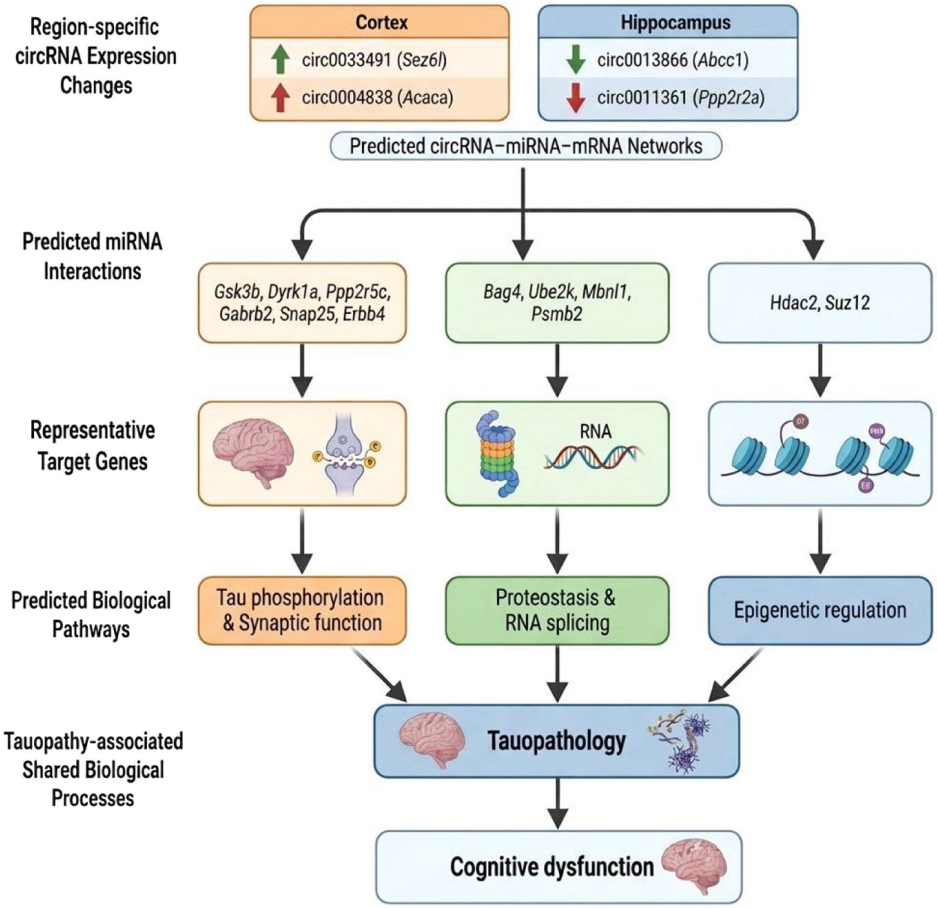


Figure 5. Conceptual framework of region-specific circRNA–miRNA–mRNA networks in tauopathy. Region-specific circRNAs prioritized from the cortex (circ0033491 and circ0013866) and hippocampus (circ0004838 and circ0011361) were associated with predicted circRNA–miRNA–mRNA networks. Representative target genes are shown as examples of molecules represented within the predicted networks. Exploratory enrichment analyses link these networks to pathways related to tau phosphorylation, synaptic function, proteostasis, RNA processing, metabolic regulation, neuroinflammation, and epigenetic regulation. These pathways were associated with common BPs relevant to tauopathy. This figure represents a hypothesis-generating framework based on computational predictions and exploratory enrichment analyses and does not imply validated mechanistic relationships.

age-associated changes relative to the 3-month baseline; therefore, direct 6M-versus-12M and cortex-versus-hippocampus differential expression analyses were not performed. Future studies incorporating these comparisons may provide additional insight into temporal and regional circRNA expression patterns. The relatively small sample size prevented assessment of sex-specific differences, and the four prioritized circRNAs were not independently validated by qRT-PCR or RNase R resistance assays. Consequently, the circRNAs identified in this study should be considered prioritized candidates for future investigation rather than validated regulators of tau pathology.

In summary, this study provides a region-specific circRNA resource for the hTau mouse model and prioritizes four candidate circRNAs, circ0033491 (*Sez6l*), circ0013866 (*Abcc1*), circ0004838 (*Acaca*), and circ0011361 (*Ppp2r2a*), for future investigation. Although exploratory, the predicted networks associated with these circRNAs highlight molecular pathways relevant to tauopathy and provide a framework for future mechanistic and functional studies.

Acknowledgments

Dr. Domenico Praticò is the Scott Richards North Star Foundation Chair for Alzheimer's research.

Funding

This research was in part supported by a grant from the National Institute on Health (AG 073622) to D.P.

Author Contributions

M.S.H.: conceptualization, experimental design, data analysis, figure preparation, and manuscript writing. D.P.: supervision, conceptualization, experimental design, conceptual guidance, manuscript review, and editing.

Conflict of Interest

The authors declare that they have no conflict of interests.

Data Availability Statement

The datasets generated and analyzed during this study are available from the corresponding author upon reasonable request.

Ethics Statement

All animal procedures were approved by the IACUC at Temple University and conducted in accordance with National Institutes of Health guidelines for the care and use of laboratory animals.

Supplementary Materials

Supplemental information can be found here: Supplementary.

References

1. Nichols E., Steinmetz J.D., Vollset S.E., Fukutaki K., Chalek J., Abd-Allah F., … Vos T. (2022). Estimation of the global prevalence of dementia in 2019 and forecasted prevalence in 2050: An analysis for the Global Burden of disease study 2019. *The Lancet Public Health* **7**(2), e105–e25. doi: 10.1016/S2468-2667(21)00249-8.
2. Spillantini M.G. & Goedert M. (2013). Tau pathology and neurodegeneration. *Lancet. Neurol.* **12**(6), 609–622. PMID: 23684085; doi: 10.1016/S1474-4422(13)70090-5.
3. You X., Vlatkovic I., Babic A., Will T., Epstein I., Tushev G., … Chen W. (2015). Neural circular RNAs are derived from synaptic genes and regulated by development and plasticity. *Nat. Neurosci.* **18**(4), 603–610. PMID: 25714049; doi: 10.1038/nn.3975.
4. Wang Y. & Mandelkow E. (2016). Tau in physiology and pathology. *Nat. Rev. Neurosci.* **17**(1), 5–21. PMID: 26631930; doi: 10.1038/nrn.2015.1.
5. Iqbal K., Liu F., & Gong C.X. (2016). Tau and neurodegenerative disease: The story so far. *Nat. Rev. Neurol.* **12**(1), 15–27. PMID: 26635213; doi: 10.1038/nrneurol.2015.225.
6. Hanger D.P., Anderton B.H., & Noble W. (2009). Tau phosphorylation: The therapeutic challenge for neurodegenerative disease. *Trends Mol. Med.* **15**(3), 112–119. PMID: 19246243; doi: 10.1016/j.molmed.2009.01.003.
7. de Calignon A., Polydoro M., Suarez-Calvet M., William C., Adamowicz D.H., Kopeikina K.J., … Hyman B.T. (2012). Propagation of tau pathology in a model of early Alzheimer's disease. *Neuron* **73**(4), 685–697. PMID: 22365544; doi: 10.1016/j.neuron.2011.11.033.
8. Braak H. & Braak E. (1991). Neuropathological stageing of Alzheimer-related changes. *Acta Neuropathol.* **82**(4), 239–259. PMID: 1759558; doi: 10.1007/BF00308809.
9. Bartel D.P. (2009). MicroRNAs: Target recognition and regulatory functions. *Cell* **136**(2), 215–233. PMID: 19167326; doi: 10.1016/j.cell.2009.01.002.
10. Wang X., Liu P., Zhu H., Xu Y., Ma C., Dai X., … Qin C. (2009). miR-34a, a microRNA up-regulated in a double transgenic mouse model of Alzheimer's disease, inhibits bcl2 translation. *Brain Res. Bull.* **80**(4–5), 268–273. PMID: 19683563; doi: 10.1016/j.brainresbull.2009.08.006.
11. Hebert S.S. & De Strooper B. (2009). Alterations of the microRNA network cause neurodegenerative disease. *Trends Neurosci.* **32**(4), 199–206. PMID: 19268374; doi: 10.1016/j.tins.2008.12.003.
12. Delay C. & Hebert S.S. (2011). MicroRNAs and Alzheimer's disease mouse models: Current insights and future research avenues. *Int. J. Alzheimers Dis.* **2011**(1), 894938. PMID: 21826259; doi: 10.4061/2011/894938.
13. Cha D.J., Mengel D., Mustapic M., Liu W., Selkoe D.J., Kapogiannis D., … Walsh D.M. (2019). miR-212 and miR-132 are downregulated in neurally derived plasma exosomes of Alzheimer's patients. *Front. Neurosci.* **13**, 1208. PMID: 31849573; doi: 10.3389/fnins.2019.01208.
14. Lauretti E., Dincer O., & Pratico D. (2021). Regional and temporal miRNAs expression profile in a transgenic mouse model of tauopathy: Implication for its pathogenesis. *Mol. Psychiatry* **26**(11), 7020–7028. PMID: 31988432; doi: 10.1038/s41380-020-0655-2.
15. Memczak S., Jens M., Elefsinioti A., Torti F., Krueger J., Rybak A., … Rajewsky N. (2013). Circular RNAs are a large class of animal RNAs with regulatory potency. *Nature* **495**(7441), 333–338. PMID: 23446348; doi: 10.1038/nature11928.
16. Rybak-Wolf A., Stottmeister C., Glazar P., Jens M., Pino N., Giusti S., … Rajewsky N. (2015). Circular RNAs in the Mammalian brain are highly abundant, conserved, and dynamically expressed. *Mol. Cell* **58**(5), 870–885. PMID: 25921068; doi: 10.1016/j.molcel.2015.03.027.
17. Hansen T.B., Jensen T.I., Clausen B.H., Bramsen J.B., Finsen B., Damgaard C.K., & Kjems J. (2013). Natural RNA circles function as efficient microRNA sponges. *Nature* **495**(7441), 384–388. PMID: 23446346; doi: 10.1038/nature11993.
18. Salmena L., Poliseno L., Tay Y., Kats L., & Pandolfi P.P. (2011). A ceRNA hypothesis: The Rosetta Stone of a hidden RNA language? *Cell* **146**(3), 353–358. PMID: 21802130; doi: 10.1016/j.cell.2011.07.014.
19. Piwecka M., Glazar P., Hernandez-Miranda L.R., Memczak S., Wolf S.A., Rybak-Wolf A., … Rajewsky N. (2017). Loss of a mammalian circular RNA locus causes miRNA deregulation and affects brain function. *Science* **357**(6357), eaam8526. PMID: 28798046; doi: 10.1126/science.aam8526.
20. Dube U., Del-Aguila J.L., Li Z., Budde J.P., Jiang S., Hsu S., … Cruchaga C. (2019). An atlas of cortical circular RNA expression in Alzheimer disease brains demonstrates clinical and pathological associations. *Nat. Neurosci.* **22**(11), 1903–1912. PMID: 31591557; doi: 10.1038/s41593-019-0501-5.
21. Gao Y., Takenaka K., Santucci K., Lindner G., Xu S.M., Cheng Y., & Janitz M. (2025). Dysregulated circRNA-miRNA-mRNA networks reveal stage-specific mRNA expression changes in Parkinson's disease. *Mol. Brain* **19**(1), 4. PMID: 41327336; doi: 10.1186/s13041-025-01262-2.
22. Hanan M., Simchovitz A., Yayon N., Vaknine S., Cohen-Fultheim R., Karmon M., … Kadener S. (2020). A Parkinson's disease CircRNAs Resource reveals a link between circSLC8A1 and oxidative stress. *EMBO Mol. Med.* **12**(11), e13551. PMID: 33438831; doi: 10.15252/emmm.202013551.
23. Gong C.X., Grundke-Iqbal I., & Iqbal K. (1994). Dephosphorylation of Alzheimer's disease abnormally phosphorylated tau by protein phosphatase-2A. *Neuroscience* **61**(4), 765–772. PMID: 7838376; doi: 10.1016/0306-4522(94)90400-6.
24. Graff J., Rei D., Guan J.S., Wang W.Y., Seo J., Hennig K.M., … Tsai L.H. (2012). An epigenetic blockade of cognitive functions in the neurodegenerating brain. *Nature* **483**(7388), 222–226. PMID: 22388814; doi: 10.1038/nature10849.
25. Brown G.C. & Neher J.J. (2014). Microglial phagocytosis of live neurons. *Nat. Rev. Neurosci.* **15**(4), 209–216. PMID: 24646669; doi: 10.1038/nrn3710.
26. Sekar S. & Liang W.S. (2019). Circular RNA expression and function in the brain. *Noncoding RNA Res.* **4**(1), 23–29. PMID: 30891534; doi: 10.1016/j.ncrna.2019.01.001.
27. Dong X., Bai Y., Liao Z., Gritsch D., Liu X., Wang T., … Scherzer C.R. (2023). Circular RNAs in the human brain are tailored to neuron identity and neuropsychiatric disease [Preprint]. *BioRxiv*. PMID: 37066229; doi: 10.1101/2023.04.01.535194.
28. Chung D.C., Roemer S., Petrucelli L., & Dickson D.W. (2021). Cellular and pathological heterogeneity of primary tauopathies. *Mol. Neurodegener.* **16**(1), 57. PMID: 34425874; doi: 10.1186/s13024-021-00476-x.
29. Broekaart D.W.M., Sharma A., Ramakrishnan A., Chongtham A., Gunther D.M., Subramaniyan S., … Pereira A.C. (2025). Molecular signatures of regional vulnerability to tauopathy in excitatory cortical neurons. *Acta Neuropathol.* **149**(1), 60. PMID: 40481857; doi: 10.1007/s00401-025-02879-2.
30. Dharshini S.A.P., Taguchi Y.H., & Gromiha M.M. (2019). Investigating the energy crisis in Alzheimer disease using transcriptome study. *Sci. Rep.* **9**(1), 18509. PMID: 31811163; doi: 10.1038/s41598-019-54782-y.
31. Wang B.Z., Yang J.J., Zhang H., Smith C.A., & Jin K. (2019). AMPK signaling regulates the age-related decline of hippocampal neurogenesis. *Aging Dis.* **10**(5), 1058–1074. PMID: 31595203; doi: 10.14336/AD.2019.0102.
32. Chakraborty P., Ibanez de Opakua A., Purslow J.A., Fromm S.A., Chatterjee D., Zachrdla M., … Zweckstetter M. (2024). GSK3beta phosphorylation catalyzes the aggregation of tau into Alzheimer's disease-like filaments. *Proc. Natl. Acad. Sci. U. S. A.* **121**(52), e2414176121. PMID: 39693350; doi: 10.1073/pnas.2414176121.

33. Drewes G., Lichtenberg-Kraag B., Doring F., Mandelkow E.M., Biernat J., Goris J., … Mandelkow E. (1992). Mitogen activated protein (MAP) kinase transforms tau protein into an Alzheimer-like state. *EMBO J.* **11**(6), 2131–2138. PMID: 1376245; doi: 10.1002/j.1460-2075.1992.tb05272.x.

34. Sayas C.L. & Avila J. (2021). GSK-3 and Tau: A key duet in Alzheimer's disease. *Cells* **10**(4), 721. PMID: 33804962; doi: 10.3390/cells10040721.

35. Luo S., Liu H., Xiao T., Li Y., Liu X., Xiao X., … Shen L. (2026). Neuronal PPP2R5C in plasma is a potential biomarker for early diagnosis of Alzheimer's disease. *Cell Rep. Med.* **7**(3), 102631. PMID: 41720088; doi: 10.1016/j.xcrm.2026.102631.

36. Sontag J.M. & Sontag E. (2014). Protein phosphatase 2A dysfunction in Alzheimer's disease. *Front. Mol. Neurosci.* **7**, 16. PMID: 24653673; doi: 10.3389/fnmol.2014.00016.

37. Brinkmalm A., Brinkmalm G., Honer W.G., Frolich L., Hausner L., Minthon L., … Ohrfelt A. (2014). SNAP-25 is a promising novel cerebrospinal fluid biomarker for synapse degeneration in Alzheimer's disease. *Mol. Neurodegener.* **9**, 53. PMID: 25418885; doi: 10.1186/1750-1326-9-53.

38. Klaassen R.V., Stroeder J., Coussen F., Hafner A.S., Petersen J.D., Renancio C., … Smit A.B. (2016). Shisa6 traps AMPA receptors at postsynaptic sites and prevents their desensitization during synaptic activity. *Nat. Commun.* **7**, 10682. PMID: 26931375; doi: 10.1038/ncomms10682.

39. Li H., Fan Y., Chen C., Xu Y., Wang X., & Liu W. (2025). Identification of GABBR2 as a diagnostic marker and its association with Abeta in Alzheimer's disease. *Biochem. Biophys. Rep.* **42**, 102035. PMID: 40927314; doi: 10.1016/j.bbrep.2025.102035.

40. Rasmussen A.H., Rasmussen H.B., & Silahtaroglu A. (2017). The DLGAP family: Neuronal expression, function and role in brain disorders. *Mol. Brain* **10**(1), 43. PMID: 28870203; doi: 10.1186/s13041-017-0324-9.

41. Jiang S., Srikanth M., Serpe R., Yavari S., Gaur P., Collins G.A., … Myeku N. (2025). Early proteasome downregulation and dysfunction drive proteostasis failure in Alzheimer's disease. *Brain* **148**(12), 4372–4388. PMID: 40488453; doi: 10.1093/brain/awaf222.

42. Song S. & Jung Y.K. (2004). Alzheimer's disease meets the ubiquitin-proteasome system. *Trends Mol. Med.* **10**(11), 565–570. PMID: 15519283; doi: 10.1016/j.molmed.2004.09.005.

43. Yoon B.H., Kim J., Sengupta S., Park C.J., Ko M., Kang J.H., … Lee M.S. (2025). Targeted autophagic clearance of Tau protects against Alzheimer's disease through amelioration of Tau-mediated lysosomal stress. *Theranostics* **15**(17), 9240–9260. PMID: 40963907; doi: 10.7150/thno.118409.

44. Xu K., Dai X.L., Huang H.C., & Jiang Z.F. (2011). Targeting HDACs: A promising therapy for Alzheimer's disease. *Oxid. Med. Cell Longev.* **2011**(1), 143269. PMID: 21941604; doi: 10.1155/2011/143269.

45. Carpentier C., Ghanem D., Fernandez-Gomez F.J., Jumeau F., Philippe J.V., Freyermuth F., … Caillet-Boudin M.L. (2014). Tau exon 2 responsive elements deregulated in myotonic dystrophy type I are proximal to exon 2 and synergistically regulated by MBNL1 and MBNL2. *Biochim. Biophys. Acta* **1842**(4), 654–664. PMID: 24440524; doi: 10.1016/j.bbadis.2014.01.004.

46. Berrocal M. & Mata A.M. (2023). The plasma membrane Ca(2+)-ATPase, a molecular target for tau-induced cytosolic calcium dysregulation. *Neuroscience* **518**, 112–118. PMID: 35469971; doi: 10.1016/j.neuroscience.2022.04.016.

47. Melchior B., Mittapalli G.K., Lai C., Duong-Polk K., Stewart J., Guner B., … Yazici Y. (2019). Tau pathology reduction with SM07883, a novel, potent, and selective oral DYRK1A inhibitor: A potential therapeutic for Alzheimer's disease. *Aging Cell* **18**(5), e13000. PMID: 31267651; doi: 10.1111/acel.13000.

48. Rosenberger A.F., Rozemuller A.J., van der Flier W.M., Scheltens P., van der Vies S.M., & Hoozemans J.J. (2014). Altered distribution of the EphA4 kinase in hippocampal brain tissue of patients with Alzheimer's disease correlates with pathology. *Acta Neuropathol. Commun.* **2**, 79. PMID: 25027113; doi: 10.1186/s40478-014-0079-9.

49. Woo R.S., Lee J.H., Yu H.N., Song D.Y., & Baik T.K. (2010). Expression of ErbB4 in the apoptotic neurons of Alzheimer's disease brain. *Anat. Cell Biol.* **43**(4), 332–339. PMID: 21267408; doi: 10.5115/acb.2010.43.4.332.

50. Sun Y., Wang Y., Chen S.T., Chen Y.J., Shen J., Yao W.B., … Chen S. (2020). Modulation of the astrocyte-neuron lactate shuttle system contributes to neuroprotective action of fibroblast growth factor 21. *Theranostics* **10**(18), 8430–8445. PMID: 32724479; doi: 10.7150/thno.44370.

51. Trabjerg M.S., Morkholt A.S., Lichota J., Oklinski M.K.E., Andersen D.C., Jonsson K., … Nieland J.D.V. (2020). Dysregulation of metabolic pathways by carnitine palmitoyl-transferase 1 plays a key role in central nervous system disorders: Experimental evidence based on animal models. *Sci. Rep.* **10**(1), 15583. PMID: 32973137; doi: 10.1038/s41598-020-72638-8.

52. Walker D.G., Whetzel A.M., & Lue L.F. (2015). Expression of suppressor of cytokine signaling genes in human elderly and Alzheimer's disease brains and human microglia. *Neuroscience* **302**, 121–137. PMID: 25286386; doi: 10.1016/j.neuroscience.2014.09.052.

53. Deng Y., Li B., Liu Y., Iqbal K., Grundke-Iqbal I., & Gong C.X. (2009). Dysregulation of insulin signaling, glucose transporters, O-GlcNAcylation, and phosphorylation of tau and neurofilaments in the brain: Implication for Alzheimer's disease. *Am. J. Pathol.* **175**(5), 2089–2098. PMID: 19815707; doi: 10.2353/ajpath.2009.090157.

54. Rosenberger A.F., Hilhorst R., Coart E., Garcia Barrado L., Naji F., Rozemuller A.J., … van derVies S.M. (2016). Protein kinase activity decreases with higher Braak stages of Alzheimer's disease pathology. *J. Alzheimers Dis.* **49**(4), 927–943. PMID: 26519433; doi: 10.3233/JAD-150429.

55. Shomali T. & Trempe J.F. (2026). Targeting of kinases to treat neurodegenerative diseases. *Pharmacol. Rev.* **78**(3), 100128. PMID: 41880688; doi: 10.1016/j.pharmr.2026.100128.

56. Gong C.X., Shaikh S., Wang J.Z., Zaidi T., Grundke-Iqbal I., & Iqbal K. (1995). Phosphatase activity toward abnormally phosphorylated tau: Decrease in Alzheimer disease brain. *J Neurochem.* **65**(2), 732–738. PMID: 7616230; doi: 10.1046/j.1471-4159.1995.65020732.x.

57. Levenga J., Krishnamurthy P., Rajamohamedsait H., Wong H., Franke T.F., Cain P., … Hoeffer C.A. (2013). Tau pathology induces loss of GABAergic interneurons leading to altered synaptic plasticity and behavioral impairments. *Acta Neuropathol. Commun.* **1**, 34. PMID: 24252661; doi: 10.1186/2051-5960-1-34.

58. Mattson M.P. (2020). Involvement of GABAergic interneuron dysfunction and neuronal network hyperexcitability in Alzheimer's disease: Amelioration by metabolic switching. *Int. Rev. Neurobiol.* **154**, 191–205. PMID: 32739004; doi: 10.1016/bs.irn.2020.01.006.

59. Smeralda C.L., Pandit S., Turrini S., Reilly J., Palmisano A., Sprugnoli G., … Santarnecchi E. (2024). The role of parvalbumin interneuron dysfunction across neurodegenerative dementias. *Ageing Res. Rev.* **101**, 102509. PMID: 39306248; doi: 10.1016/j.arr.2024.102509.

60. Colom-Cadena M., Spires-Jones T., Zetterberg H., Blennow K., Caggiano A., DeKosky S.T., … Catalano S.M. (2020). Synaptic health endpoints working G. The clinical promise of biomarkers of synapse damage or loss in Alzheimer's disease. *Alzheimers Res. Ther.* **12**(1), 21. PMID: 32122400; doi: 10.1186/s13195-020-00588-4.

61. DeKosky S.T. & Scheff S.W. (1990). Synapse loss in frontal cortex biopsies in Alzheimer's disease: Correlation with cognitive severity. *Ann. Neurol.* **27**(5), 457–464. PMID: 2360787; doi: 10.1002/ana.410270502.

62. Ittner L.M., Ke Y.D., Delerue F., Bi M., Gladbach A., van Eersel J., … Gotz J. (2010). Dendritic function of tau mediates amyloid-beta toxicity in Alzheimer's disease mouse models. *Cell* **142**(3), 387–397. PMID: 20655099; doi: 10.1016/j.cell.2010.06.036.

63. Karunanayake C. & Page R.C. (2021). Cytosolic protein quality control machinery: Interactions of Hsp70 with a network of co-chaperones and substrates. *Exp. Biol. Med. (Maywood)* **246**(12), 1419–1434. PMID: 33730888; doi: 10.1177/1535370221999812.

64. Minoia M., Boncoraglio A., Vinet J., Morelli F.F., Brunsting J.F., Poletti A., … Carra S. (2014). BAG3 induces the sequestration of proteasomal clients into cytoplasmic puncta: Implications for a proteasome-to-autophagy switch. *Autophagy* **10**(9), 1603–1621. PMID: 25046115; doi: 10.4161/auto.29409.

65. Chesser A.S., Pritchard S.M., & Johnson G.V. (2013). Tau clearance mechanisms and their possible role in the pathogenesis of Alzheimer disease. *Front. Neurol.* **4**, 122. PMID: 24027553; doi: 10.3389/fneur.2013.00122.

66. Wang L., Sooram B., Kumar R., Schedin-Weiss S., Tjernberg L.O., & Winblad B. (2025). Tau degradation in Alzheimer's disease: Mechanisms and therapeutic opportunities. *Alzheimers Dement.* **21**(3), e70048. PMID: 40109019; doi: 10.1002/alz.70048.

67. Goniotaki D., Hausherr M., Lynham S., Ale A., Chennell G., Marcotti S., … Srivastava D.P. (2025). Proteomic analysis links truncated tau to lysosome motility, autophagy, and endo-lysosomal dysfunction. *Alzheimers Dement.* **21**(12), e70977. PMID: 41399158; doi: 10.1002/alz.70977.

68. Piras A., Collin L., Gruninger F., Graff C., & Ronnback A. (2016). Autophagic and lysosomal defects in human tauopathies: Analysis of post-mortem brain from patients with familial Alzheimer disease, corticobasal degeneration and progressive supranuclear palsy. *Acta Neuropathol. Commun.* **4**, 22. PMID: 26936765; doi: 10.1186/s40478-016-0292-9.

69. Guan J.S., Haggarty S.J., Giacometti E., Dannenberg J.H., Joseph N., Gao J., … Tsai L.H. (2009). HDAC2 negatively regulates memory formation and synaptic plasticity. *Nature* **459**(7243), 55–60. PMID: 19424149; doi: 10.1038/nature07925.

70. von Schimmelmann M., Feinberg P.A., Sullivan J.M., Ku S.M., Badimon A., Duff M.K., … Schaefer A. (2016). Polycomb repressive complex 2 (PRC2) silences genes responsible for neurodegeneration. *Nat. Neurosci.* **19**(10), 1321–1330. PMID: 27526204; doi: 10.1038/nn.4360.

71. Wang C., Fan L., Khawaja R.R., Liu B., Zhan L., Kodama L., … Gan L. (2022). Microglial NF-kappaB drives tau spreading and toxicity in a mouse model of tauopathy. *Nat. Commun.* **13**(1), 1969. PMID: 35413950; doi: 10.1038/s41467-022-29552-6.

72. Vogels T., Murgoci A.N., & Hromadka T. (2019). Intersection of pathological tau and microglia at the synapse. *Acta Neuropathol. Commun.* **7**(1), 109. PMID: 31277708; doi: 10.1186/s40478-019-0754-y.

73. Ising C., Venegas C., Zhang S., Scheiblich H., Schmidt S.V., Vieira-Saecker A., … Heneka M.T. (2019). NLRP3 inflammasome activation drives tau pathology. *Nature* **575**(7784), 669–673. PMID: 31748742; doi: 10.1038/s41586-019-1769-z.

74. Pampuscenko K., Morkuniene R., Krasauskas L., Smirnovas V., Brown G.C., & Borutaite V. (2023). Extracellular tau stimulates phagocytosis of living neurons by activated microglia via Toll-like 4 receptor-NLRP3 inflammasome-caspase-1 signalling axis. *Sci. Rep.* **13**(1), 10813. PMID: 37402829; doi: 10.1038/s41598-023-37887-3.

75. Li G., Xu J., Tian X., Xiao J., Long J., Chen Y., … Zhao S. (2025). Efferocytosis: The art of cellular clearance and novel perspectives in disease therapy. *Mol. Cancer* **24**(1), 268. PMID: 41126210; doi: 10.1186/s12943-025-02484-7.

76. Chen Y., Kou Y., Ni Y., Yang H., Xu C., Fan H., & Liu H. (2025). Microglia efferocytosis: An emerging mechanism for the resolution of neuroinflammation in Alzheimer's disease. *J. Neuroinflammation* **22**(1), 96. PMID: 40159486; doi: 10.1186/s12974-025-03428-0.

77. Zhao J., Zhang W., Wu T., Wang H., Mao J., Liu J., … Wang Q. (2021). Efferocytosis in the central nervous system. *Front. Cell Dev. Biol.* **9**, 773344. PMID: 34926460; doi: 10.3389/fcell.2021.773344.

78. Liu F. & Gong C.X. (2008). Tau exon 10 alternative splicing and tauopathies. *Mol. Neurodegener.* **3**, 8. PMID: 18616804; doi: 10.1186/1750-1326-3-8.

79. Shi J., Qian W., Yin X., Iqbal K., Grundke-Iqbal I., Gu X., … Liu F. (2011). Cyclic AMP-dependent protein kinase regulates the alternative splicing of tau exon 10: A mechanism involved in tau pathology of Alzheimer disease. *J. Biol. Chem.* **286**(16), 14639–14448. PMID: 21367856; doi: 10.1074/jbc.M110.204453.